

## ORIGINAL ARTICLE

## LSD1 controls metastasis of androgen-independent prostate cancer cells through PXN and LPAR6

A Ketscher<sup>1,2</sup>, CA Jilg<sup>1</sup>, D Willmann<sup>1</sup>, B Hummel<sup>1</sup>, A Imhof<sup>3</sup>, V Rüsseler<sup>1</sup>, S Hölz<sup>1,2</sup>, E Metzger<sup>1</sup>, JM Müller<sup>1</sup> and R Schüle<sup>1,4,5</sup>

Lysine-specific demethylase 1 (LSD1) was shown to control gene expression and cell proliferation of androgen-dependent prostate cancer (PCa) cells, whereas the role of LSD1 in androgen-independent metastatic prostate cancer remains elusive. Here, we show that depletion of LSD1 leads to increased migration and invasion of androgen-independent PCa cells. Transcriptome and cistrome analyses reveal that LSD1 regulates expression of *lysophosphatidic acid receptor 6 (LPAR6)* and cytoskeletal genes including the focal adhesion adaptor protein paxillin (PXN). Enhanced LPAR6 signalling upon LSD1 depletion promotes migration with concomitant phosphorylation of PXN. In mice LPAR6 overexpression enhances, whereas knockdown of LPAR6 abolishes metastasis of androgen-independent PCa cells. Taken together, we uncover a novel mechanism of how LSD1 controls metastasis and identify LPAR6 as a promising therapeutic target to treat metastatic prostate cancer.

*Oncogenesis* (2014) 3, e120; doi:10.1038/oncsis.2014.34; published online 6 October 2014

## INTRODUCTION

Prostate cancer (PCa) is the second leading cause of cancer deaths in men worldwide.<sup>1</sup> In early clinical stages, PCa is confined to the prostate and can be cured by surgery and/or radiotherapy. However, in 20–53% of the cases relapse occurs within the first 5 years.<sup>2</sup> A large proportion of these patients initially responds to hormone ablation therapy, but develops androgen-independent PCa that finally metastasizes locally or distantly. Currently, there are no therapies for these patients that prevent metastasis.

Formation of metastases requires tumour cell migration and invasion. Migration is a tightly regulated process involving cell polarisation, site-specific extracellular signalling, cell protrusion, as well as the coordinated attachment to and detachment from the extracellular matrix.<sup>3</sup> The latter is mainly mediated by focal adhesions (FAs), large protein complexes primarily located at the leading edge of migrating cells. During cell protrusion, FA turnover enables cells to reattach at new positions. FAs are built of proteins including paxillin (PXN), talin 1 (TLN1), zyxin (ZYG) and the regulatory subunit 2 beta of phosphoinositide-3-kinase (PIK3R2). In response to extracellular signals such as lysophosphatidic acid (LPA), PXN is phosphorylated at tyrosine 118 (Y118) by a complex consisting of FA-Kinase (FAK) and Src.<sup>4</sup> Previous studies showed that overexpression of PXN, TLN1, ZYG or PIK3R2 increases cell migration and/or metastasis in various cancer types including PCa.<sup>5–8</sup>

LPA binds to G protein-coupled transmembrane receptors that are divided in two subgroups, the endothelial differentiation gene family (LPAR1–3) and the purinergic receptor-related family (LPAR4–6). Consequences on LPA signalling are diverse and only partially understood, as distinct pathways are activated depending on cell and receptor type.<sup>9,10</sup>

In addition to regulation of FAs by signalling events, expression of genes encoding FA constituents is transcriptionally controlled. In general, gene regulation requires cooperation of transcription

factors and cofactors including histone modifying enzymes such as lysine-specific demethylase 1 (LSD1 or KDM1A). LSD1 is an amine oxidase that specifically demethylates H3K4me2/me1<sup>11</sup> or H3K9me2/me1,<sup>12</sup> thereby affecting target gene transcription. To date, there are no data describing a role for LSD1 in the regulation of focal adhesion-associated proteins in PCa. Altered LSD1 levels were correlated with different types of cancer.<sup>12,13</sup> In PCa cells LSD1 promotes transcription in cooperation with the androgen receptor and is required for proliferation in an androgen-dependent manner.<sup>12</sup> In breast cancer, LSD1 was reported to control the expression of epithelial–mesenchymal transition-related genes as part of the NuRD complex.<sup>14</sup> It is not known whether a similar mechanism accounts for LSD1-controlled metastases formation in PCa.

Here, we show that LSD1 regulates a LPAR6-FA signalling network. LSD1 directly controls transcription of numerous focal adhesion and cytoskeleton-associated genes. Depletion of LSD1 activates LPA signalling by upregulation of LPAR6 along with phosphorylation of PXN resulting in increased migration of androgen-independent PCa cells. Furthermore, in mice LPAR6 depletion dramatically impairs the formation of metastases. Taken together, we describe a novel mechanism controlling the metastatic behaviour of PCa cells and identify LPAR6 as a promising target to prevent metastasis of androgen-independent PCa.

## RESULTS

LSD1 controls migration and invasion of androgen-independent PCa cells

To investigate a potential role of LSD1 in androgen-independent PCa, we first tested the effect of RNAi-mediated knockdown of LSD1 on the androgen receptor-negative cell lines PC-3M-luc and DU145. We monitored migration, invasion and proliferation in

<sup>1</sup>Urologische Klinik und Zentrale Klinische Forschung, Klinikum der Universität Freiburg, Freiburg, Germany; <sup>2</sup>Universität Freiburg, Fakultät für Biologie, Freiburg, Germany;

<sup>3</sup>Adolf-Butenandt Institut und Munich Center of Integrated Protein Science (CIPS), Ludwig-Maximilians-Universität München, München, Germany; <sup>4</sup>BIOS Centre of Biological Signaling Studies, Albert-Ludwigs-University, Freiburg, Germany and <sup>5</sup>Deutsches Konsortium für Translationale Krebsforschung (DKTK), Standort, Freiburg, Germany.

Correspondence: Professor R Schüle, Urologische Klinik und Zentrale Klinische Forschung, Uniklinik Freiburg, Breisacherstrasse 66, 79106 Freiburg, Germany.

E-mail: roland.schuele@uniklinik-freiburg.de

Received 14 May 2014; revised 5 August 2014; accepted 17 August 2014

real-time by measuring cell-mediated impedance on a microelectrode array, which is displayed by the cell index. Migration and invasion of both cell lines was strongly increased upon knockdown of LSD1 compared to cells treated with unrelated control siRNA (Figures 1a and c). Vice versa, we observed impaired migration when LSD1 was overexpressed in PC-3M-luc cells using a lentivirus-driven construct (Figures 1d and e). In comparison, proliferation was not influenced by knockdown of LSD1 (Supplementary Figures S1a and b). Overexpression of LSD1 only marginally influenced proliferation (Supplementary Figure S1c). Thus, LSD1 controls the migratory and invasive behaviour of androgen-independent PCa cells.

LSD1 directly regulates transcription of cytoskeleton-associated genes

To identify genes that mediate the effect of LSD1 on PCa cell migration and invasion, we performed transcriptome analysis. RNA from PC-3M-luc cells treated with either siRNA against LSD1 or unrelated control was isolated and subjected to massive parallel sequencing (RNA-sequencing). Bioinformatic analyses showed that 1355 genes were differentially regulated upon knockdown of LSD1 (Figure 2a). DAVID gene ontology analysis revealed that knockdown of LSD1 in PC-3M-luc cells affects genes that are linked to the proteasome complex, to centromere and kinetochore of chromosomes and to the basolateral plasma membrane.

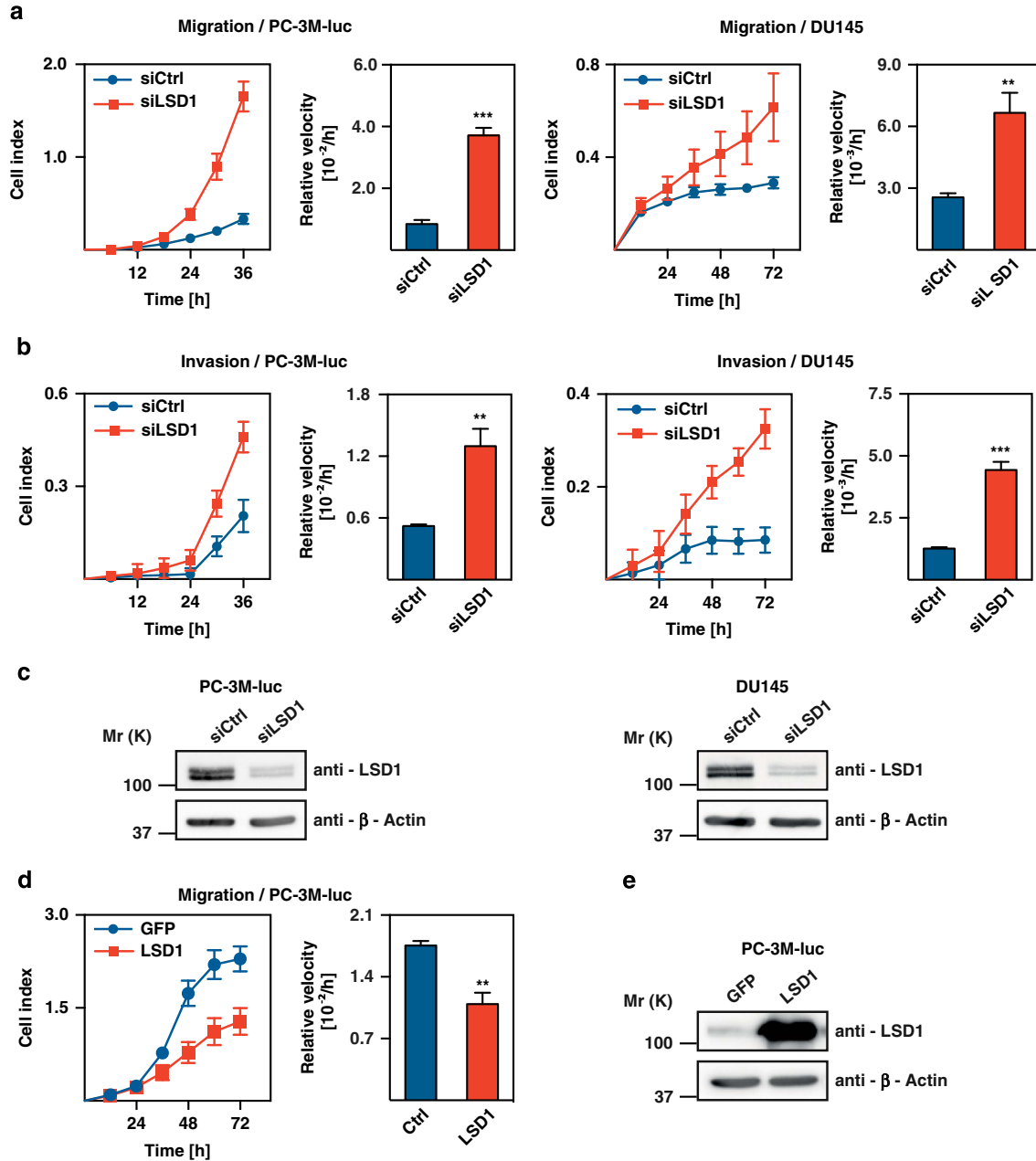


**Figure 1.** LSD1 controls migration and invasion of androgen-independent prostate cancer cell lines. Migration (a) and invasion (b) assays of PC-3M-luc and DU145 cells treated with siRNA against LSD1 (siLSD1) or unrelated control siRNA (siCtrl). (d) Migration assay of PC-3M-luc cells overexpressing LSD1. PC-3M-luc cells were infected with either control- (GFP) or LSD1-expressing lentivirus (LSD1). (a, b, d) Cell indices and relative velocities are shown. (c, e) Levels of LSD1 were analysed by western blots decorated with the indicated antibodies.  $\beta$ -Actin was used as loading control.  $n \geq 3$ . Error bars represent  $\pm$  s.d. or  $+s.d.$   $**P \leq 0.01$ ,  $***P \leq 0.001$ .

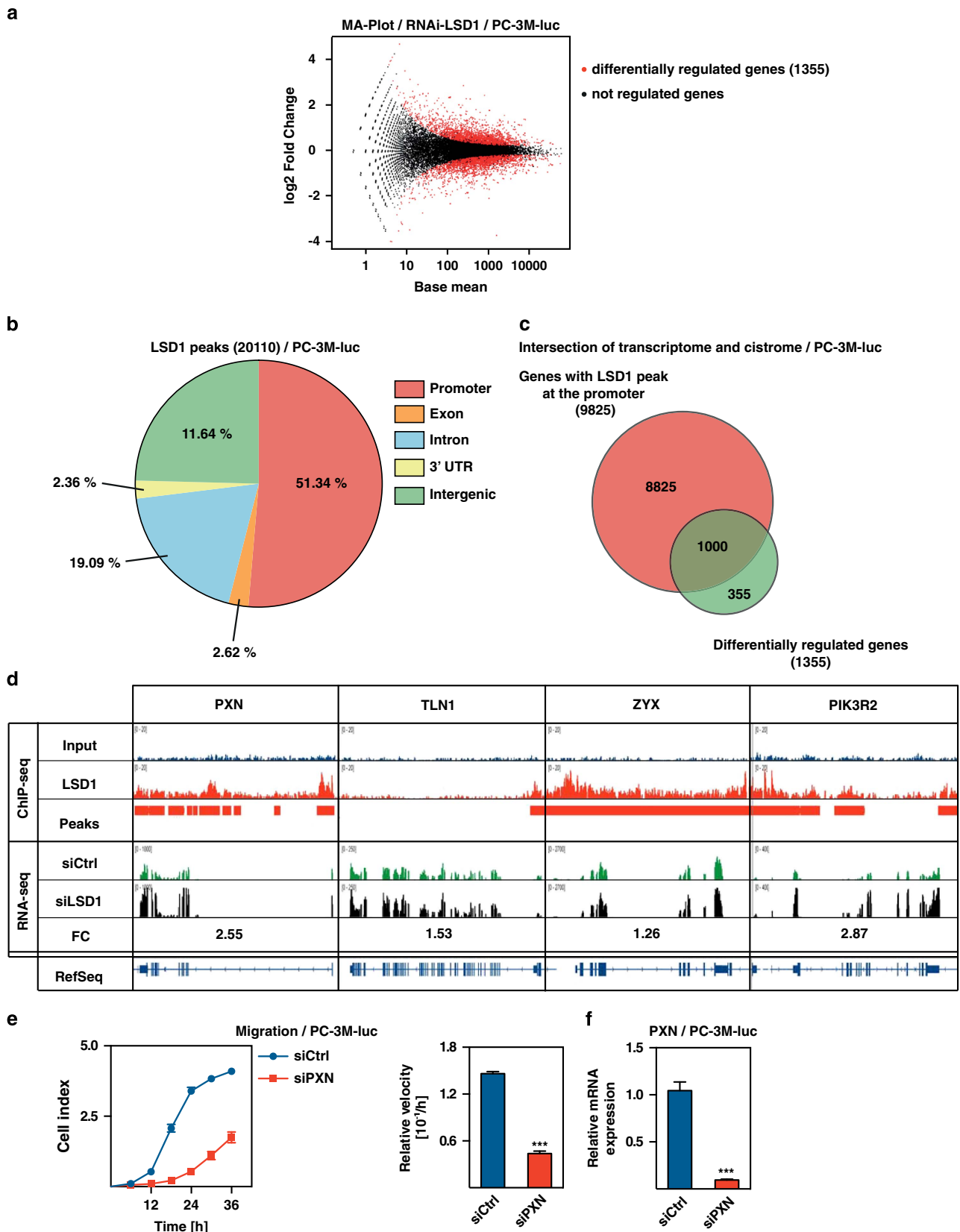


**Figure 2.** LSD1 directly regulates the expression of cytoskeleton-associated genes. **(a)** MA-Plot representing the differentially regulated genes (red dots) in PC-3M-luc cells upon knockdown of LSD1. **(b)** Pie chart displaying genomic distribution of LSD1 peaks in PC-3M-luc cells determined by ChIP-sequencing analysis. **(c)** Venn diagram, showing the intersection between differentially regulated genes upon knockdown of LSD1 and genes with LSD1 peaks at the promoter. **(d)** Localisation of LSD1 peaks (ChIP-sequencing) and read coverage (RNA-sequencing) at PXN, TLN1, ZYX and PIK3R2. FC: Fold Change. **(e)** Migration assay of PC-3M-luc cells treated with siRNA against PXN or control siRNA. Cell index and relative velocity are shown. **(f)** mRNA levels of PXN were analysed by qRT-PCR.  $n \geq 3$ . Error bars represent  $\pm$  s.d. or  $\pm$  s.d. \*\*\* $P \leq 0.001$ .

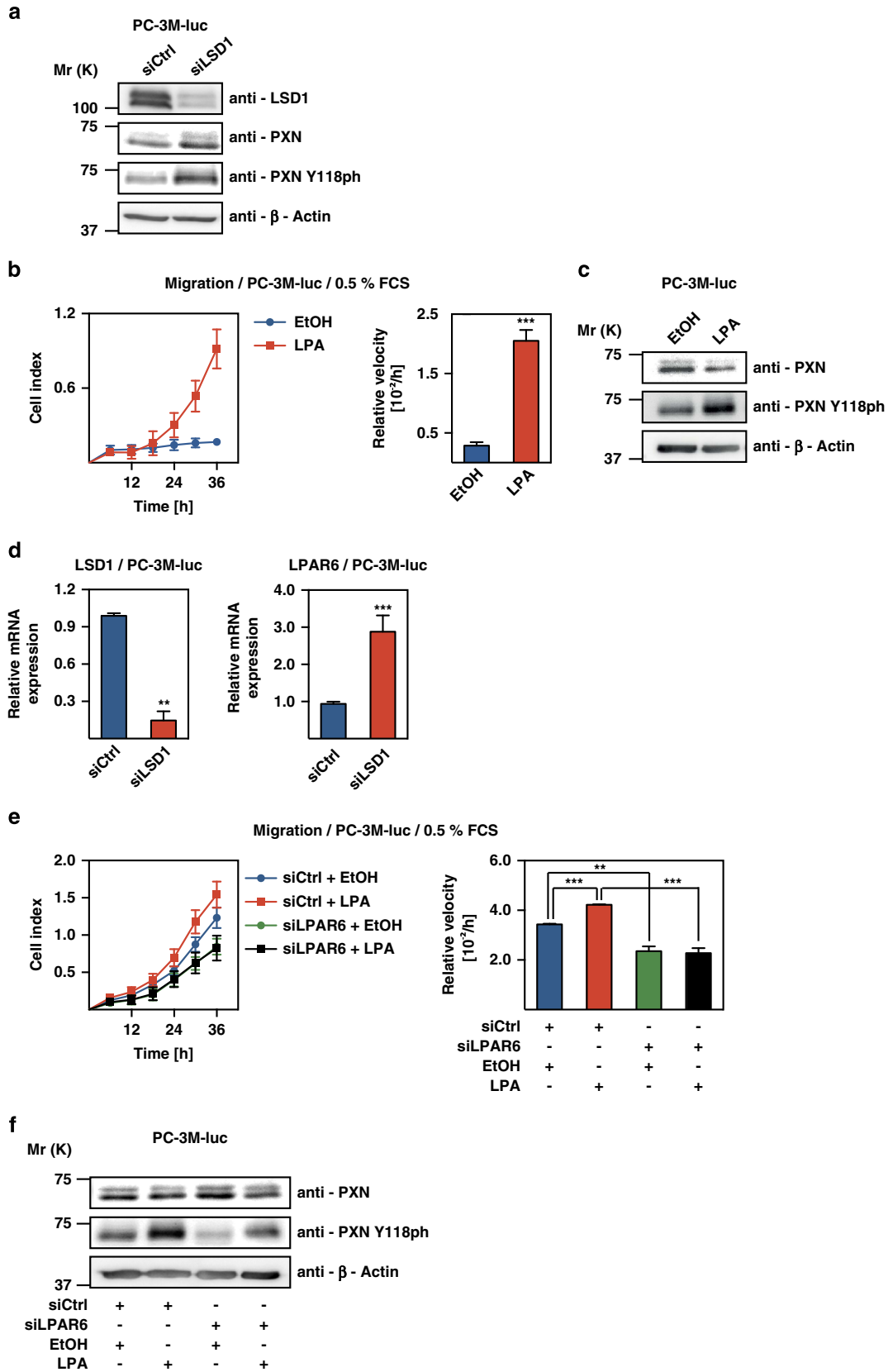


**Figure 3.** LPAR6 mediates LSD1-controlled migration. **(a)** Levels of PXN and PXN Y118ph. **(b)** Migration assay of PC-3M-luc cells treated with LPA or Ethanol (EtOH). **(d)** mRNA levels of LPAR6 were analysed by qRT-PCR. **(e)** Migration assay of PC-3M-luc cells treated with LPA or EtOH and transfected with siRNA against LPAR6 or an unrelated control siRNA. **(g)** Migration assay of PC-3M-luc cells treated with siRNA either against LSD1, LPAR6 or both. **(h)** mRNA levels of LSD1 and LPAR6 were analysed by qRT-PCR. **(i)** Migration assay of PC-3M-luc cells overexpressing LPAR6. **(b, e, g, i)** Cell indices and relative velocities are shown. **(a, c, f, k)** Levels of LSD1, PXN, and PXN Y118ph were analysed by western blots decorated with the indicated antibodies.  $\beta$ -Actin was used as loading control.  $n \geq 3$ . Error bars represent  $\pm$ s.d. or  $\pm$ s.d.  $*P \leq 0.05$ ,  $**P \leq 0.01$ ,  $***P \leq 0.001$ .

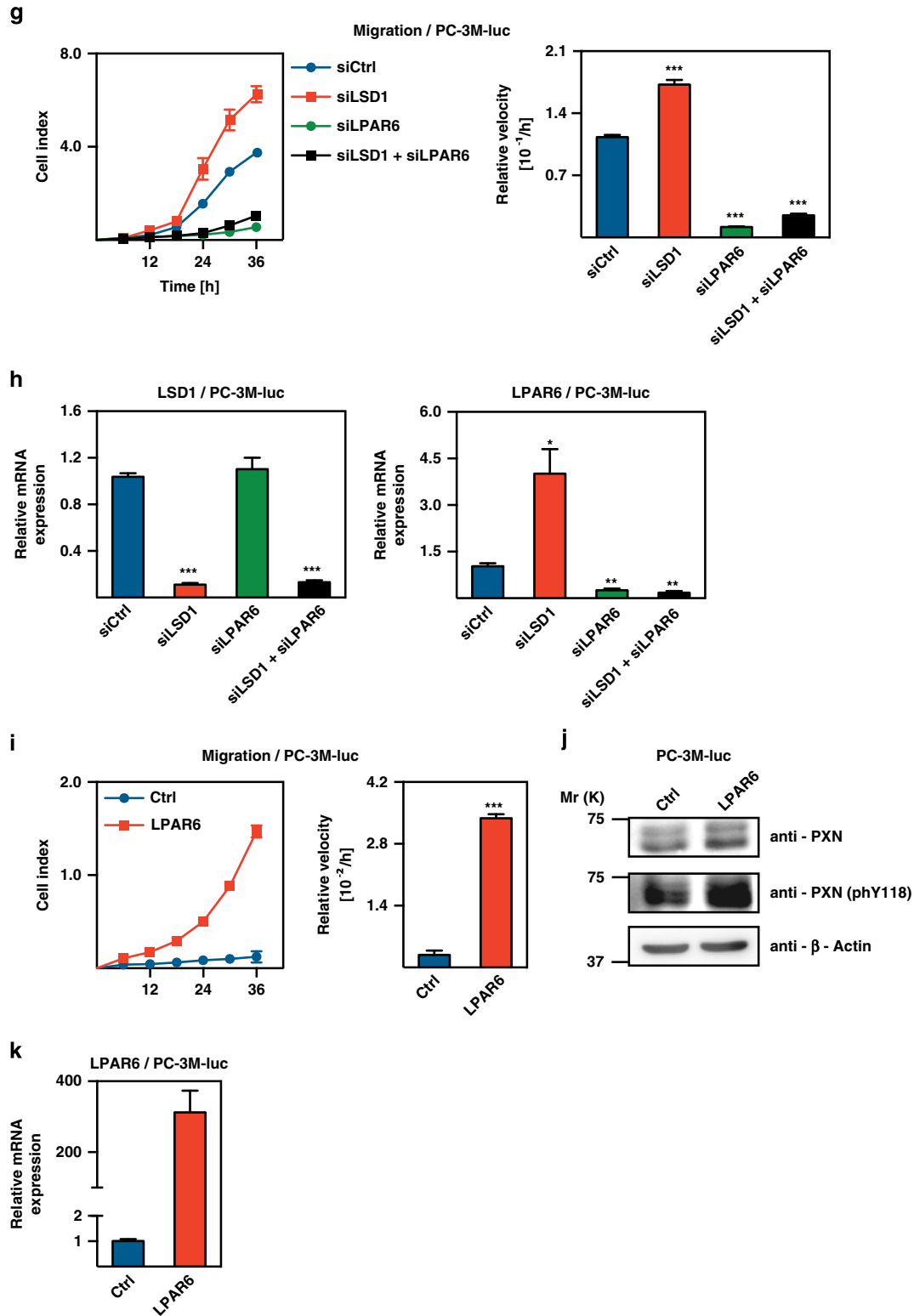
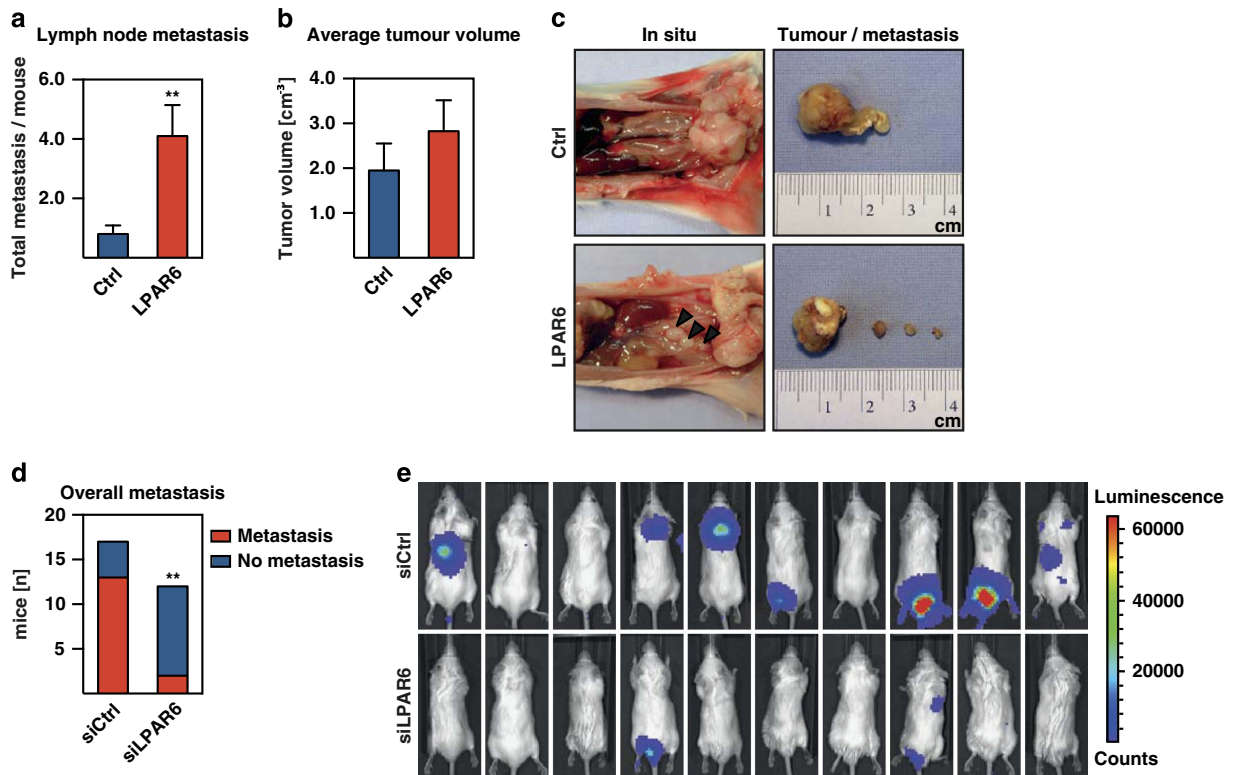


Figure 3. Continued.

Interestingly, 148 (10.9%) differentially regulated genes were part of the cytoskeleton-associated gene cluster, potentially accounting for the migratory phenotype (Supplementary Figure S2a).

To determine which of the cytoskeleton-associated genes are direct LSD1 targets, we conducted chromatin immunoprecipitation assay with LSD1 antibody in PC-3M-luc cells followed by massive parallel sequencing (ChIP-sequencing). 20110

high-confidence LSD1 peaks were identified, with 51.34% located at the promoter ( $\pm 2500$  bp around the transcription start site) of 9825 genes (Figure 2b). Intersection of LSD1 transcriptome and cistrome revealed 1000 differentially regulated genes with LSD1 promoter occupancy (Figure 2c). The intersection comprised 110 of the 148 cytoskeleton-associated genes. Of these 110 genes 66 were downregulated and 44 upregulated (Supplementary Table 2).



**Figure 4.** LPAR6 controls migration and metastasis. Number of metastases (**a**) and tumour volume (**b**) in an orthotopic tumour model of the mouse prostate were analysed. PC-3M-luc cells overexpressing LPAR6 (LPAR6) or control cells (Ctrl) were injected. (**c**) Macroscopic view of tumours and lymph node metastases.  $n = 10$  mice. Error bars represent  $\pm$ s.e.m. (**d**) Decreased overall metastases in mice injected with PC-3M-luc cells after LPAR6 knockdown into the lateral tail vein. (**e**) Bioluminescent images taken after 28 days show metastases of PC-3M-luc cells transfected with siRNA against LPAR6 (siLPAR6;  $n = 12$ ) or unrelated control siRNA (siCtrl;  $n = 17$ ). Statistics were done using Fisher's exact test.  $**P \leq 0.01$ .

The reorganisation of the cytoskeleton is required for efficient cell migration.<sup>15</sup> Thus, the deregulation of contributing proteins such as FA components can lead to aberrant cell migration. Interestingly, FA components such as PXN, TLN1, ZYX and PIK3R2 were upregulated upon knockdown of LSD1, which was confirmed by quantitative reverse transcription-PCR and western blot (Figure 2d, Supplementary Figures S2b and c). Although other differentially regulated genes could also contribute to the migratory phenotype upon knockdown of LSD1, we focused on focal adhesion components to track LSD1-controlled migration. These data indicate that LSD1 directly regulates cytoskeleton-associated genes, thereby accounting for the migratory behaviour of androgen-independent PCa cells.

To provide further evidence, that these genes are mediators of LSD1-controlled cell migration, we treated PC-3M-luc cells with siRNA against these FA constituents. Knockdown of PXN, TLN1, ZYX or PIK3R2 severely impaired migration of PC-3M-luc cells (Figures 2e and f, Supplementary Figures S2d and e). In accordance with our data, upregulation of PXN, TLN1, ZYX and PIK3R2 was previously correlated with enhanced cell motility in different types of cancer.<sup>5–8</sup> In summary, as exemplified by key components of FAs, we demonstrate that enhanced cell migration upon LSD1 knockdown is mediated through direct regulation of cytoskeleton-associated genes.

LPAR6 signalling induces phosphorylation of PXN after LSD1 knockdown

Next, we investigated the influence of LSD1 knockdown on FA signalling. Previous studies showed that phosphorylation of PXN at Y118 (PXN Y118ph) is necessary for disassembly of FAs.<sup>16</sup> Western blot analysis of PC-3M-luc cell lysate upon knockdown of

LSD1 revealed increased levels of PXN and PXN Y118ph (Figure 3a). Phosphorylation of PXN occurs upon mechanical force, integrin clustering or activation of growth factor receptors by their ligands.<sup>17</sup> Furthermore, phosphorylation of PXN is detected upon activation of LPA signalling in PC-3 cells.<sup>4,18–20</sup> Therefore, we investigated the impact of LPA on migration of androgen-independent PCa cells. Treatment of serum-starved PC-3M-luc cells with LPA resulted in increased PXN Y118ph levels and migration (Figures 3b and c). LPA signals through binding to the LPAR family members LPAR1–6.<sup>10</sup> Our RNA-sequencing data showed that LPAR1, 2, 3 and 6 were expressed in PC-3M-luc cells. From these receptors only LPAR6 was differentially regulated upon knockdown of LSD1 (Supplementary Figures S3a and b). However, LSD1 depletion did not influence expression of the RB1 gene, which is transcribed from the opposite DNA strand of the LPAR6 locus. CHIP-sequencing analysis showed that LPAR6 is not a direct target of LSD1. We confirmed upregulation of LPAR6 by quantitative reverse transcription-PCR (Figure 3d) owing to the low quality of commercially available antibodies against LPAR6. These data suggest that LPAR6 is a major mediator of LPA signalling in androgen-independent PCa cells. In favour of this idea, knockdown of LPAR6 decreased migration of PC-3M-luc cells (Figure 3e). Furthermore, after LPAR6 knockdown, LPA no longer stimulated migration of PC-3M-luc cells (Figure 3e) and PXN Y118ph was reduced (Figure 3f).

To provide further evidence that increased migration and elevated levels of PXN Y118ph upon knockdown of LSD1 are dependent on LPAR6, we treated PC-3M-luc cells with siRNA against LSD1 or LPAR6, either alone or in combination. Indeed, increased migration upon knockdown of LSD1 was not observed in LPAR6-depleted PC-3M-luc cells (Figures 3g and h). Comparable

results were obtained in DU145 cells (Supplementary Figures S3c and d).

Next, we investigated the effect of elevated LPAR6 levels on migration of androgen-independent PCa cells. Overexpression of LPAR6 increased migration of PC-3M-luc cells (Figure 3i) and phosphorylation of PXN Y118ph (Figure 3j). Elevated mRNA expression of LPAR6 upon induction with doxycycline was confirmed by quantitative reverse transcription-PCR (Figure 3k). To demonstrate that the LPAR6-mediated increase in migration requires activation of FAs, we knocked down PXN in PC-3M-luc cells overexpressing LPAR6. Whereas overexpression of LPAR6 led to elevated migration of PC-3M-luc cells, simultaneous depletion of PXN completely abrogated the observed phenotype (Supplementary Figures S3e and f). Together, these results show that LPAR6 and its downstream effector PXN are upregulated upon knockdown of LSD1, thereby enhancing migration. Furthermore, our data demonstrate that LSD1-controlled migration of androgen-independent PCa cells in response to LPA is mediated by LPAR6.

#### LPAR6 controls metastasis of androgen-independent PCa cells

Our *in vitro* data suggest that metastasis of androgen-independent PCa depends on LPAR6. To address this issue *in vivo*, we used an orthotopic prostate tumour model. PC-3M-luc cells stably overexpressing LPAR6 were injected into the dorsal lobe of the prostate of immunodeficient mice. Five weeks after injection, tumour size and number of lymph node metastases were analysed. Importantly, elevated levels of LPAR6 led to a significantly increased number of lymph node metastases compared to the control group (Figures 4a and c). In comparison, tumour volumes were not significantly affected (Figures 4b and c). Tumours as well as lymph node metastases were verified by histological staining (Supplementary Figure S4a). To further support the role of LPAR6 in metastasis, we used a second *in vivo* metastasis model, in which PCa cells extravasate from the blood vessel system to form distant metastases. LPAR6-overexpressing PC-3M-luc cells were injected into the lateral tail vein of immunodeficient mice and metastases formation was monitored by bioluminescence over 5 weeks and verified by histological staining. LPAR6 overexpression led to a dramatically increased number of metastases (Supplementary Figures S4b–e). Together, the results of both models clearly show that LPAR6 controls metastasis of androgen-independent PCa cells.

To evaluate whether LPAR6 may serve as therapeutic target for the treatment of metastatic PCa, we monitored metastases formation upon knockdown of LPAR6 *in vivo*. Therefore, we injected PC-3M-luc cells transfected with siRNA against LPAR6 or an unrelated control siRNA into the lateral tail vein of immunodeficient mice (Supplementary Figure S4f). To ensure the stability of LPAR6 depletion we monitored mRNA levels over 8 days post transfection (Supplementary Figure S4g). Compared to control mice, the number of metastases was significantly lower in mice injected with LPAR6-depleted cells (Figures 4d and e and Supplementary Figure S4h) demonstrating that LPAR6 is crucial for metastasis of PC-3M-luc cells. Taken together, our data imply that inhibition of LPAR6 signalling is a novel and promising strategy to prevent metastasis of androgen-independent PCa.

#### DISCUSSION

In the present study, we uncovered a novel mechanism for LSD1-controlled migration of androgen-independent PCa cells and identified LPAR6 as a promising target for PCa therapy. Transcriptome and cistrome data sets provided in this manuscript for androgen-independent PCa cells reveal that LSD1 is a direct regulator of genes of the LPAR6-FA signalling network such as PXN, TLN1, ZYX and PIK3R2. This mechanism of migration control is different from the one previously observed in breast cancer

cells, where LSD1 was reported to interact with the NuRD-complex and to regulate epithelial–mesenchymal transition-related genes such as *TGFB1*, *LMNB2*, *IGF1R*, *EGFR*, *CCND2*, *ADK*, *PSEN1*, *RHOA*, *FGF21* and *APAF1*.<sup>14</sup> In contrast, we neither observe interaction of LSD1 with NuRD components nor regulation of these epithelial–mesenchymal transition-related genes in PC-3M-luc cells upon knockdown of LSD1. Thus, LSD1 appears to control cancer cell migration by different mechanisms in distinct types of cancer.

The role of LSD1 in PCa that is described here differs from that in androgen-dependent PCa cells. There, LSD1 cooperates with the androgen receptor to control androgen-dependent gene expression and proliferation. In contrast, we could not observe severe effects of LSD1 knockdown or overexpression on proliferation of PC-3M-luc and DU145 cells. It will be interesting to evaluate the diverse roles of LSD1 in PCa that is either androgen receptor-dependent or -independent.

LPAR6 was previously shown to be highly expressed in tumour tissue and metastases of human hepatocellular carcinoma compared to normal liver,<sup>21</sup> but the function of LPAR6 was not investigated. Our data show that overexpression of LPAR6 leads to increased migration and metastasis of PC-3M-luc and DU145 cells. In comparison, Liu *et al.* observed that transgenic mice expressing LPAR1-3, members of the endothelial differentiation gene family, under the control of the mouse mammary tumour virus-promoter developed mammary tumours and metastases.<sup>22</sup> Importantly, we demonstrate that LPAR6 depletion dramatically decreases the metastatic potential of androgen-independent PCa cells in mice. Our findings uncover LPAR6 as the first member of the purinergic receptor-related family as a promising target for the treatment of androgen-independent PCa. Our correlation of LPAR6 expression with metastasis suggests that LPAR6 antagonizing compounds might be of therapeutic value to prevent metastasis. Based on treatment with LPA antagonists, previous studies implicated LPAR1 in migration of androgen-independent PCa cells.<sup>23</sup> However, in these studies observations were neither verified by knockdown of LPAR1 nor the role of LPAR6 was taken into account. Furthermore, the authors only tested the impact of LPA antagonists directed against members of the endothelial differentiation gene family on migration. In comparison, LPAR6 belongs to the purinergic receptor-related gene family, and the effects of current, low-specificity, LPAR inhibitors on all family members have only partially been documented. Further evaluation of the therapeutic potential of the individual LPAR family members requires the development of novel inhibitors with high affinity and specificity. In addition, the development of specific and high quality antibodies against LPAR6 will provide insights into expression pattern of LPAR6 in different stages of PCa. Taken together, our analyses demonstrate that LSD1 is as a key regulator of the LPAR6-FA signalling network and identify LPAR6 as a novel potential therapeutic target for the treatment of androgen-dependent metastatic PCa.

#### MATERIALS AND METHODS

##### Plasmids

Expression plasmids for LSD1 and LPAR6 were generated by LR11 recombination according to the supplier (Gateway, Invitrogen, Carlsbad, CA, USA) using entry clones (GeneCopia, Rockville, MD, USA; GC-I0048-CF; accession number NM\_001162498; pENTR-D-TOPO-LSD1, Schüle Laboratory, Freiburg, Germany) and either a puromycin-selectable and doxycycline-inducible pRTS plasmid55 (modified to contain a Gateway cassette, V5 and His-tag epitope) or FU-GFP vector (kindly provided by Owen Witte, UCLA, Los Angeles, CA, USA). Vectors without insert were used as control.

##### Cell culture and transfection

PC-3M-luc cells and DU145 cells were cultured in EMEM (Lonza, Basel, Switzerland, 12–125) supplemented with 10% FCS, 1% L-glutamine (Lonza, BE17-605E) and 1% penicillin-streptomycin (Lonza, DE17-602E). RNAi knockdown was performed using Dharmafect 2 (Thermo Scientific,

Waltham, MA, USA, T-2002-01) in PC-3M cells and Dharmafect 4 (Thermo Scientific, T-2004-01) in DU145 cells using 25 nM siRNA according to the manufacturer's instruction. For knockdown of LSD1 the following siRNAs were used: siCtrl: 5'-AACGTACGCGGAATCTTCGA-3' and siLSD1 5'-acacaaggaaag cuagaaga-3'. For others siCtrl 5'-GAAAGTCCTAGAT CCACACGCAAT-3', siLPA6 5'-UCAGCAUGGUGUUUGUGCUUGGGUU-3', siPXN 5'-CATACCCAACTGGAAACCACACATA-3', siTLN1 5'-CATTGTACTTGAT ACGGCCAGTGAT-3', siZYX 5'-CAGGAGAAAGGTGAGCAGTATTGAT-3' and siPIK3R2 5'-CCCTCAGGAAAGGCGGGAACAATA-3'. Dharmafect Duo (Thermo Scientific, T-2010-01) was used for plasmid transfection as described in the manual. Puromycin (Sigma, St Louis, MO, USA, P8733, 5 µg/ml) was administered to cells 24 h post transfection. 293T cells were cultured in DMEM supplemented with 10% FCS, 1% L-glutamine and 1% penicillin-streptomycin. Viral production was performed as described.<sup>12</sup> PC-3M cells were infected with FU-GFP or FU-GFP-LSD1 and subjected to migration assay 24 h post transduction.

### Western blot analysis and Immunoprecipitation

Experiments were performed as described.<sup>12</sup> Antibodies against the following proteins were used for western blots: LSD1 (Schüle Laboratory, 3544), β-Actin (Sigma, A1978), PXN (Cell Signaling, Danvers, MA, USA, 2542), PXN Y118ph (Cell Signaling, 2541), TLN1 (AbD Serotec, Kidlington, UK, MCA4770), ZYX (Abcam, Cambridge, UK, ab71842), PIK3R2 (Abcam, ab28356). Western blots for pPXN (Y118) were performed 90 min post LPA induction (Figures 3b and f), 72 h after treatment with siRNA against LSD1 (Figure 3a) or 24 h post transfection with LPA6 overexpressing construct (Figure 3j).

### Cell proliferation, migration and invasion assays

Prior to the experiment PC-3M-luc cells were treated for 24 h with siRNA or for 48 h with doxycycline (2 µg/ml), respectively. LPA (Cayman, Ann Arbor, MI, USA, 10010093) was added immediately before starting the assay to overnight serum-starved cells at a concentration of 10 µM and after serum starvation overnight. Proliferation, cell migration and invasion were monitored using the xCelligence system (Roche, Basel, Switzerland) that measures electrode impedance upon cell attachment to the surface of proliferation (E-plate) or migration (CIM-plate) chambers. For invasion, transwell chamber filters were coated with matrigel (BD Biosciences, Franklin Lakes, NJ, USA, 354230) diluted 1:40 in EMEM medium. For proliferation  $5 \times 10^3$  PC-3M cells and  $1 \times 10^4$  DU145 cells were seeded into E-plate 16. For migration and invasion PC-3M cells were seeded at  $5 \times 10^4$  and DU145 cells at  $1 \times 10^4$  into the transwell containing 0.5% FCS EMEM in the upper chamber and 10% FCS EMEM in the lower chamber. Cell indices display electrode impedance and were automatically recorded every 15 min by the xCelligence system software (Roche). Relative velocities represent the change of the cell index over time.

### RNA extraction and semiquantitative reverse transcription-PCR

RNA isolation and quantitative PCR after reverse transcription were performed as described.<sup>12</sup> For normalisation of expression in PC-3M-luc and DU145 cells ACTB, HPRT1 and POLR2A were used and data were related to negative control cells treated with control siRNA, empty vector or empty virus. Experiments were repeated in triplicate at least three times. Primers are shown in Supplementary Table I.

### RNA sequencing

RNA samples were sequenced by the standard Illumina protocol to create raw sequence files (.fastq files). We aligned these reads to the hg19 build of the human genome using TopHat version 2.<sup>24</sup> The aligned reads were counted with the Homer software (analyzeRNA) and DEG's were identified using EdgeR<sup>25</sup> and DESeq version 1.8.3.<sup>26</sup> Only differentially regulated genes with a *P*-value  $\leq 10^{-5}$  were included in our analysis.

### ChIP sequencing

Chromatin immunoprecipitation experiments were performed using the antibody against LSD1 (Abcam, ab17721, lot GR 79477-1) on protein A-Sepharose 4B (GE Healthcare, Chalfont St Giles, UK) essentially as described.<sup>27</sup> Libraries were prepared from immunoprecipitated DNA according to standard methods. ChIP-Seq libraries were sequenced using a HiSeq 2000 (Illumina, San Diego, CA, USA) and mapped to the hg19 reference genome using Bowtie 0.12.7.<sup>28</sup> Data were further analyzed using

the peak finding algorithm MACS 1.4<sup>29</sup> using input as control. All peaks with FDR bigger than 1% were excluded from further analysis. The uniquely mapped reads were used to generate the genome-wide intensity profiles, which were visualized using the IGV genome browser.<sup>30</sup> HOMER<sup>31</sup> was used to annotate peaks, calculate overlaps between different peak files and for motif searches. The genomic features (promoter ( $\pm 2500$  bp from transcription start site), exon, intron, 3' UTR and intergenic regions) were defined and calculated using Refseq and HOMER, respectively. To draw the average gene profile CEAS was used.<sup>32</sup> Genes annotated by HOMER were further used for a DAVID analysis.<sup>33</sup>

### In vivo metastasis assay

All mice were housed in the pathogen-free barrier facility of the University Medical Center Freiburg in accordance with institutional guidelines and approved by the regional board. Seven to eight-week-old male C.B-17.Cg-Prkdc<sup>scid</sup> Lyst<sup>bg</sup>/Crl-mice (Charles River, Wilmington, MA, USA) were used for *in vivo* metastasis assays. In all,  $1 \times 10^6$  PC-3M-luc cells were resuspended in 100 µl PBS or 20 µl matrigel and injected either into the lateral tail vein or the dorsal lobe of the mouse prostate. For bioluminescent imaging mice were anesthetized with isoflurane (Forene, Abbott GmbH, Chicago, IL, USA) and 150 µg/g D-Luciferin (Caliper Life Science, Hopkinton, MA, USA, 119222) was injected intraperitoneal. Two minutes after injection bioluminescence was imaged for 30 s to 5 min at day 7, 14, 21 and 28 of the experiment. At day 28 mice were sacrificed and organs with luminescent signals were collected for HE staining. For the orthotopic metastasis model primary tumors and axillary lymph nodes were dissected after 28 days.

### Statistical analysis

If not otherwise stated, significance was calculated using an unpaired *t*-test and data were shown as mean  $\pm$  s.d. or  $\pm$  s.d.

### CONFLICT OF INTEREST

The authors declare no conflict of interest.

### ACKNOWLEDGEMENTS

We thank G Bornkamm (GSF, Munich) and O Witte (UCLA, Los Angeles) for providing plasmids. We are obliged to Astrid Rieder for providing excellent technical assistance. We thank Holger Greschik and David McGarry for critical reading of the manuscript. This work was supported by DFG Grants SFB 850, 992, 746 Schu688/9-1, 10-2, 11-2, 12-1 and ERC-2012-AdGrant 322844-LSD1 to RS.

### AUTHOR CONTRIBUTIONS

AK, CAJ, EM and RS designed experiments; AK, CAJ, EM, VR, AI and SH performed research; AK, CAJ, EM, DW, BH, AI, JMM and RS analyzed data; and AK, CAJ, JMM, EM and RS wrote and edited the manuscript.

### REFERENCES

- 1 American Cancer Society Cancer Facts & Figure 2013. Available from: <http://www.cancer.org/research/cancerfactsstatistics/cancerfactsfigures2013/index> (cited 2013 Sep 29).
- 2 Han M, Partin AW, Zahurak M, Piantadosi S, Epstein JI, Walsh PC. Biochemical (prostate specific antigen) recurrence probability following radical prostatectomy for clinically localized prostate cancer. *J Urol* 2003; **169**: 517–523.
- 3 Ridley AJ, Schwartz MA, Burridge K, Firtel RA, Ginsberg MH, Borisy G *et al*. Cell migration: integrating signals from front to back. *Science* 2003; **302**: 1704–1709.
- 4 Saito J, Morishige N, Chikama T-I, Gu J, Sekiguchi K, Nishida T. Differential regulation of focal adhesion kinase and paxillin phosphorylation by the small GTP-binding protein Rho in human corneal epithelial cells. *Jpn J Ophthalmol* 2004; **48**: 199–207.
- 5 Azuma K, Tanaka M, Uekita T, Inoue S, Yokota J, Ouchi Y *et al*. Tyrosine phosphorylation of paxillin affects the metastatic potential of human osteosarcoma. *Oncogene* 2005; **24**: 4754–4764.
- 6 Pellinen T, Rantala JK, Arjonen A, Mpindi J-P, Kallioniemi O, Ivaska J. A functional genetic screen reveals new regulators of β1-integrin activity. *J Cell Sci* 2012; **125**: 649–661.
- 7 Sy SM-H, Lai PB-S, Pang E, Wong NL-Y, To K-F, Johnson PJ *et al*. Novel identification of zyxin upregulations in the motile phenotype of hepatocellular carcinoma. *Mod Pathol* 2006; **19**: 1108–1116.

- 8 Cortés I, Sánchez-Ruiz J, Zuluaga S, Calvanese V, Marqués M, Hernández C *et al*. p85 $\beta$  phosphoinositide 3-kinase subunit regulates tumor progression. *Proc Natl Acad Sci USA* 2012; **109**: 11318–11323.
- 9 Houben AJS, Moolenaar WH. Autotaxin and LPA receptor signaling in cancer. *Cancer Metastasis Rev* 2011; **30**: 557–565.
- 10 Choi JW, Herr DR, Noguchi K, Yung YC, Lee C-W, Mutoh T *et al*. LPA receptors: subtypes and biological actions. *Annu Rev Pharmacol Toxicol* 2010; **50**: 157–186.
- 11 Shi Y, Lan F, Matson C, Mulligan P, Whetstone JR, Cole PA *et al*. Histone demethylation mediated by the nuclear amine oxidase homolog LSD1. *Cell* 2004; **119**: 941–953.
- 12 Metzger E, Wissmann M, Yin N, Müller JM, Schneider R, Peters AHFM *et al*. LSD1 demethylates repressive histone marks to promote androgen-receptor-dependent transcription. *Nature* 2005; **437**: 436–439.
- 13 Lim S, Metzger E, Schüle R, Kirfel J, Buettner R. Epigenetic regulation of cancer growth by histone demethylases. *Int J Cancer* 2010; **127**: 1991–1998.
- 14 Wang Y, Zhang H, Chen Y, Sun Y, Yang F, Yu W *et al*. LSD1 is a subunit of the NuRD complex and targets the metastasis programs in breast cancer. *Cell* 2009; **138**: 660–672.
- 15 Mitra SK, Hanson DA, Schlaepfer DD. Focal adhesion kinase: in command and control of cell motility. *Nat Rev Mol Cell Biol* 2005; **6**: 56–68.
- 16 Webb DJ, Donais K, Whitmore LA, Thomas SM, Turner CE, Parsons JT *et al*. FAK-Src signalling through paxillin, ERK and MLCK regulates adhesion disassembly. *Nat Cell Biol* 2004; **6**: 154–161.
- 17 Brown MC, Turner CE. Paxillin: adapting to change. *Physiol Rev* 2004; **84**: 1315–1339.
- 18 Park JJ, Rubio MV, Zhang Z, Um T, Xie Y, Knoepf SM *et al*. Effects of lysophosphatidic acid on calpain-mediated proteolysis of focal adhesion kinase in human prostate cancer cells. *Prostate* 2012; **72**: 1595–1610.
- 19 Pasternack SM, Von Kügelgen I, Al Aboud K, Lee Y-A, Rüschemdorf F, Voss K *et al*. G protein-coupled receptor P2Y5 and its ligand LPA are involved in maintenance of human hair growth. *Nat Genet* 2008; **40**: 329–334.
- 20 Park EY, Kazlauskas A. Primary human endothelial cells secrete agents that reduce responsiveness to lysophosphatidic acid (LPA). *Biosci Rep* 2012; **32**: 393–400.
- 21 Sokolov E, Eheim AL, Ahrens WA, Walling TL, Swet JH, McMillan MT *et al*. Lysophosphatidic acid receptor expression and function in human hepatocellular carcinoma. *J Surg Res* 2013; **180**: 104–113.
- 22 Liu S, Umezū-Goto M, Murph M, Lu Y, Liu W, Zhang F *et al*. Expression of Autotaxin and Lysophosphatidic Acid Receptors Increases Mammary Tumorigenesis, Invasion, and Metastases. *Cancer Cell* 2009; **15**: 539–550.
- 23 Hao F, Tan M, Xu X, Han J, Miller DD, Tigyi G *et al*. Lysophosphatidic acid induces prostate cancer PC3 cell migration via activation of LPA1, p42 and p38 $\alpha$ . *Biochim Biophys Acta* 2007; **1771**: 883–892.
- 24 Trapnell C, Hendrickson DG, Sauvageau M, Goff L, Rinn JL, Pachter L. Differential analysis of gene regulation at transcript resolution with RNA-seq. *Nat Biotechnol* 2013; **31**: 46–53.
- 25 Robinson MD, Smyth GK. Small-sample estimation of negative binomial dispersion, with applications to SAGE data. *Biostatistics* 2008; **9**: 321–332.
- 26 Anders S, Huber W. Differential expression analysis for sequence count data. *Genome Biol* 2010; **11**: R106.
- 27 Metzger E, Yin N, Wissmann M, Kunowska N, Fischer K, Friedrichs N *et al*. Phosphorylation of histone H3 at threonine 11 establishes a novel chromatin mark for transcriptional regulation. *Nat Cell Biol* 2008; **10**: 53–60.
- 28 Langmead B, Trapnell C, Pop M, Salzberg SL. Ultrafast and memory-efficient alignment of short DNA sequences to the human genome. *Genome Biol* 2009; **10**: R25.
- 29 Zhang Y, Liu T, Meyer CA, Eeckhoute J, Johnson DS, Bernstein BE *et al*. Model-based analysis of ChIP-Seq (MACS). *Genome Biol* 2008; **9**: R137.
- 30 Thorvaldsdóttir H, Robinson JT, Mesirov JP. Integrative Genomics Viewer (IGV): high-performance genomics data visualization and exploration. *Brief Bioinformatics* 2012; **14**: 178–192.
- 31 Heinz S, Benner C, Spann N, Bertolino E, Lin YC, Laslo P *et al*. Simple combinations of lineage-determining transcription factors prime cis-regulatory elements required for macrophage and B cell identities. *Molecular Cell* 2010; **38**: 576–589.
- 32 Shin H, Liu T, Manrai AK, Liu XS. CEAS: cis-regulatory element annotation system. *Bioinformatics* 2009; **25**: 2605–2606.
- 33 Huang DW, Sherman BT, Lempicki RA. Systematic and integrative analysis of large gene lists using DAVID bioinformatics resources. *Nat Protoc* 2009; **4**: 44–57.



*Oncogenesis* is an open-access journal published by Nature Publishing Group. This work is licensed under a Creative Commons Attribution-NonCommercial-NoDerivs 4.0 International License. The images or other third party material in this article are included in the article's Creative Commons license, unless indicated otherwise in the credit line; if the material is not included under the Creative Commons license, users will need to obtain permission from the license holder to reproduce the material. To view a copy of this license, visit <http://creativecommons.org/licenses/by-nc-nd/4.0/>

Supplementary Information accompanies this paper on the *Oncogenesis* website (<http://www.nature.com/oncsis>)